Eur. Phys. J. Plus (2017) **132**: 69
DOI 10.1140/epjp/i2017-11337-8

THE EUROPEAN PHYSICAL JOURNAL PLUS

Regular Article

Carbon plants nutrition and global food security[⋆,⋆⋆]

Luigi Mariani[a]

Lombardy Museum of Agricultural History, Università degli Studi di Milano - Disaa, Via Giuseppe Celoria, 2, 20133 Milano, Italy

Received: 19 December 2016
Published online: 15 February 2017 –

Abstract. To evaluate the effects of carbon nutrition on agricultural productivity, a physiological-process–based crop simulation model, driven by the 1961–1990 monthly climate data from global FAO dataset, was developed and applied to four crops (wheat, maize, rice and soybean —WMRS) which account for 64% of the global caloric consumption of humans. Five different temperatures and CO_2 scenarios (current; glacial; pre-industrial; future_1 with 560 ppmv for CO_2 and +2 °C for temperature; and future_2 with 800 ppmv for CO_2 and +4 °C) were investigated. The relative values of WMRS global productions for past and future scenarios were, respectively, 49% of the present-day scenario for glacial, 82% for pre-industrial, 115% for future_1 and 124% for future_2. A sensitive growth of productivity of future scenarios (respectively to 117% and 134%) was observed if the northward shift of crops was allowed, and a strong increase was obtained without water limitation (from 151% to 157% for the five scenarios) and without biotic and abiotic stresses (from 30% to 40% for WMRS subject to the current scenario). Furthermore since the beginning of the Green Revolution (roughly happened between the '30s and the '50s of the twentieth century) production losses due to sub-optimal levels of CO_2 and to biotic and abiotic stresses have been masked by the strong technological innovation trend still ongoing, which, in the last century, led to a strong increase in the global crop production (+400%–600%). These results show the crucial relevance of the future choices of research and development in agriculture (genetics, land reclamation, irrigation, plant protection, and so on) to ensure global food security.

1 Introduction

1.1 Carbon plants nutrition

The relevance of CO_2 for ecosystems is not only related to its function of greenhouse gas but also to its role of inorganic molecule that closes the carbon cycle and acts as input for the photosynthetic process that supplies organic matter to almost all the food chains of the planet [1].

The key role of atmospheric CO_2 in plant nutrition was demonstrated for the first time by the Swiss physiologist Nicholas Theodore De Saussure who, in his seminal text in 1804, *Recherches chimiques sur la végétation* [2], demonstrated that carbon dioxide absorbed by plants comes from the atmosphere and not from soil organic matter as previously believed and is absorbed through the stomata and not through the roots. The fact remains that vegetation is prone to the Sprengel and Liebig law of the minimum, which states that plant production is constrained by the most limiting factor (*e.g.*, solar radiation, temperature, water and other nutrients, like nitrogen, potassium and phosphorus). This means that, while CO_2 increases, other factors can become limiting for growth. This concept reminds the farmer's need to ensure a suitable nutrition to crops [3] and highlights that high-input agricultures will also be better able to take advantage of high CO_2 levels than systems with minimal fertilizers that characterize many developing countries.

Since the beginning of the quaternary period, our planet has undergone a succession of cold glacial periods (about 15 in the last 2 million years) with atmospheric CO_2 at 180–200 ppmv and hot interglacials periods with CO_2 at about 280 ppmv. Furthermore since the beginning of the industrial revolution, CO_2 has significantly increased up to

⋆ Contribution to the Focus Point on "Plants for food, energy and sustainability" edited by G. Alimonti, S. Johansson, L. Mariani.

⋆⋆ Supplementary material in the form of a .pdf file available from the Journal web page at
http://dx.doi.org/10.1140/epjp/i2017-11337-8

[a] e-mail: luigi.mariani@unimi.it

the present values of about 400 ppmv, creating alarm for its possible effects on climate [4]. This latter question will be only indirectly addressed in this paper, which will instead be devoted to the analysis of the importance of CO_2 for plant nutrition and, as a consequence, for global food production.

The positive effect of increasing levels of atmospheric CO_2 on the productivity of plants initially stated by de Saussure [2] was reaffirmed in 1908 by Arrhenius [5], who wrote that *Another process which withdraws carbonic acid [carbon dioxide] from the air is the assimilation of plants. ... [If] the percentage of carbon dioxide be doubled, the absorption by the plants would also be doubled.* Menozzi and Pratolongo, in their book on vegetal chemistry in 1945 [6], presented a review on CO_2 fertilization citing the 1900 experiments by Brown and Escombe [7], who worked in a greenhouse of the Kew gardens and obtained negative results, perhaps due to the use of CO_2 with chlorine impurities. Quite positive results were, vice versa, obtained in 1904 by Demoussy [8] in Paris, in 1912 by Fischer in Germany [9], in 1913 by Kisseley in Moskow and in 1914 by Kein and Reinau [10] in Sterglitz, Germany. The above-mentioned experiments carried out in a controlled environment supported the idea, expressed for example by Tonzig and Marré [11], that the atmospheric level of CO_2 was far lower than optimal for the growth of plants. Based on this evidence, carbon fertilization has been adopted for many years in greenhouses with CO_2 values around 1000 ppmv [12].

The two macro-scale ecological phenomena of global greening and increase in the seasonal amplitude of the CO_2 cycle are fingerprints of the positive effect of the increasing levels of atmospheric CO_2 on the productivity of global vegetation. Global greening is the increase of terrestrial green biomass highlighted by satellite images and corroborated by simulation models, which show a significant growth of the net primary production in the last decades, spanning from tropical, temperate, and boreal regions and all vegetation types [13–15]. Zeng *et al.* [16] modeled linear trends from 1961 to 2010 and showed the substantial contribution to global greening of i) crops in agricultural areas of North America, Europe and Asia and ii) natural vegetation at high latitudes in response to warming and the CO_2 fertilization effect. Biomass decreases were also highlighted in some regions, like the western United States, Northeast China, Mongolia and South Australia [15]. By a quantitative point of view, Rafique *et al.* [17], working in the period 1982–2012 with a multi-model approach integrated with NDVI data from satellite remote sensing, obtained the most recent value of Net Primary Production (NPP) of $63\,\mathrm{Pg\,C\,yr^{-1}}$ and a global yearly increase of $0.214\,\mathrm{Pg\,C\,yr^{-1}}$ (significant at 99%) with a positive trend of NPP highlighted for the 80% of the global land area.

As for the increase of seasonal amplitude of CO_2, it is well known that an atmospheric CO_2 seasonal cycle, with minimum during the North Hemisphere summer and maximum during the North Hemisphere winter, is always superimposed to the positive overall trend in the atmospheric concentration of this gas. Zeng *et al.* [16] stated that, from 1961 to 2010, the growth season lengthened of about 14 days and the CO_2 seasonal amplitude increased by 15%, the main responsibles begin the mid-latitude croplands (25–60 °N) and the high-latitude natural vegetation (50–70 °N).

In a world with growing CO_2 atmospheric levels, the global vegetation production is also enhanced by the increase in the intrinsic water use efficiency (IWUE), which is the ratio of net photosynthesis to stomatal conductance. Indeed, C3 and C4 plants exposed to atmospheric CO_2 enrichment show an increase in IWUE due to reduced stomatal conductance and enhanced photosynthesis [18], as described by Levine *et al.* for wheat [19], by Allen *et al.* for maize [20], by Wang *et al.* for rice [18] and by Wang *et al.* for soybean [21]. As a consequence of these findings, Swann *et al.* [22] concluded that plant responses to increasing CO_2 reduce estimates of climate impacts on drought severity and this reduction is captured by using plant-centric rather than atmosphere-centric metrics.

1.2 Global food security

Food security has always been a vital aspect for human societies and it was one of the main triggering factors of the Neolithic revolution with the transition from ancient societies of hunter-gatherers to increasingly complex societies based on agriculture, significantly named "primary sector" [23]. Since the beginning of the industrial revolution the global agricultural output has kept the pace with a rapidly growing population, repeatedly defying Malthusian predictions of global food shortage and mass famine [24]. World population doubled during the 19th century (from around 0.8 in 1800 to about 1.6 billions in 1900) and more than quadrupled during the 20th century, up to 7.4 billions of 2016. Nevertheless world food production increased faster than population, which was obtained partially by bringing new lands under cultivation (estensification) but mostly as a result of a relevant increase in crop yield (intensification) which was the result of advances in genetics, cropping techniques and post-harvest technologies [25].

Progress in genetics was driven by the discovery of new methods in plant breeding promoted by the discovery of the laws of genetics by Gregory Mendel and more recently by the discovery of the three-dimensional structure of DNA by Watson and Creek, that opened the field of genetic engineering. Progress in crop techniques was triggered by the discovery of the laws of nutrition by physiologists of the 19th century, who promoted the adoption of synthetic fertilizers to improve plant nutrition [26]. Quite important were also the innovations in the fields of irrigation, mechanization, management of pests and diseases and systems for food conservation, transport and trade (from wholesale to retail). As a result, the world is better fed with fewer people in hunger today than in the past and undernourished people on world population drops from 50% in 1945 to 11% in 2015 while the number of undernourished people drops from 1011 million in 1991 to 792 million in 2015 [27].

Focusing on the period between 1961 and 2013, best covered by updated statistics of the FAOSTAT3 dataset [27], world's population increased by 135% (from 3.08 to 7.3 billion) while cereal production rose by 219% (from 0.877 to 2.8 billion tons) and global arable land grew only by 9% (from 1292 to 1408 Mha). As stated by Burney *et al.* [25], these statistics highlight that although agricultural production has increased both by extensification (expansion of land cultivated areas) and intensification (crop yield increase from the land already under cultivation), the gains observed since 1961 were in the main part due to intensification.

A positive role for world agricultural production was also played by the increase of CO_2 atmospheric concentration whereas, with an atmospheric CO_2 decline to pre-industrial levels, the yearly global crop production would drop by 25–40%, triggering a huge food crisis [28,29]. On the other hand, if the theory considering CO_2 as the principal knob governing Earth's temperature [30] is accepted, it should also be appreciated that, after the industrial revolution, CO_2 has played an important role in global food security, not only by ensuring better plant nutrition but also with the mitigation of the global temperatures of mid-high latitudes which, in the eighteenth and nineteenth centuries (little ice age), were often too cold to be suitable for agriculture [5,31–33].

The role of CO_2 in plants nutrition at different scales (from individual plants to the entire Earth) can be suitably dealt with the use of modeling tools. For instance, de Wit [34] analyzed photosynthesis in all aspects from energy requirements to maximal efficiency in converting carbon dioxide and water to food, concluding that the potential production of Earth could support the astonishing number of 146 billions of people. Burney *et al.* [25] stated that intensification of agriculture operated from 1961 to 2005 led to lower CO_2 emissions of 161 gigatons of carbon (GtC) compared to those that would have been issued if land expansion (extensification) was preferred to agricultural intensification in order to meet with the food and consumer goods requests by the growing world population. Furthermore, Capper *et al.* [35] in an analysis of the USA cow milk sector related to the scenarios of 1944 (extensive livestock breeding) and 2007 (intensive livestock breeding) highlighted that each kg of milk produced gave an emission of 3.66 kg of CO_2 in 1944 and only 1.35 in 2007. The above-mentioned data show that the enhancement of technology is fundamental for agriculture to meet with the objectives not only of food security but also of economic and environmental sustainability.

Parisi *et al.* [36] addressed the problem of rice productivity in Nepal with a monthly step mechanistic model which was run at current CO_2 atmospheric levels. Results showed that in the period 1977–2008 rice production without limitations due to nutrients, pests and diseases was about $6\,\mathrm{t\,ha^{-1}}$, with a remarkable inter-yearly steadiness. This value is significantly higher than the real production ($2.8\,\mathrm{t\,ha^{-1}}$) and highlights the advantages of the intensification of rice crop production for food security. The crucial question of intensification was also approached by Mauser *et al.* [37], who simulated world production of 18 globally most important agricultural food- and energy-crops for the reference period 1981–2010 by coupling the dynamic crop growth model PROMET with the agro-economic model DART-BIO. Three policies were proposed: A) optimization of crop management conditions (fertilizer, pest control, epoch of sowing, absence of harvest losses, etc.); B) optimization of cropping intensity (multiple yearly harvests fully realized); and C) optimization of the economic production potential (reallocating crops to fields where they can be grown more profitably). The results of the policies A), A)+B) and A)+B)+C) were, respectively, an increase by 79%, 118% ad 148% in crop production, which means a substantial improvement in crop production.

1.3 The aim of this work

The author proposes a modelling approach to global production of the four crops WMRS that today occupy nearly 46% of the global arable land (686 millions of hectares on a total arable surface of about 1500 millions of hectares) and account for about 64% of global caloric consumption and 58% of global dry biomass production [38]. The bulk of this production occurs in the extratropical regions where MWRS represents an even larger share of dry biomass production (68%), and where production has increased by 240% since 1965 (Supplementary Material, fig. S1). Remarkably, the harvested area of extratropical MWRS increased by less than 18% over this period, reflecting the fact that production increases were overwhelmingly associated with more productive agricultural practices rather than with the expansion of the cultivated area.

In the light of the above-mentioned aspects, five scenarios of MWRS global food production, which differ in CO_2 atmospheric levels and temperature, were investigated in order to highlight and discuss the role of CO_2 in global food security.

2 Data and methods

2.1 Climate data

The production model implemented for this work is driven by the global climate dataset of FAO [39] prepared by Leemans and Cramer and published by the IIASA [40]. The layers of the FAO climate dataset cover the whole Earth

surface with a pixel of 0.50×0.50 degrees in geographic coordinates (about 60×60 km at the equator) giving rise to raster arrays of 720×360 elements. For the reference period 1961–1990 the FAO dataset includes the average monthly precipitation total P_{m}, the average monthly temperature T_{m} and the sunshine fraction Sf. This latter variable is the percentage of time when bright sunshine is recorded during the day and it is directly linked to cloudiness, with a sky overcast for the whole period being equal to 0% of sunshine fraction.

The daily temperature range (dtr) has been estimated by the inversion of the Hargreaves model that simulates the daily global solar radiation at surface on the base of i) solar radiation at the top of the atmosphere on a plane parallel to the earth surface and ii) atmospheric transmissivity which, in turn, is estimated on the base of dtr and day of the year (doy) [41]. From T_{m} and dtr maximum and minimum temperatures T_{x} and T_{n} are obtained.

2.2 Model overview

The model simulates the dry matter cascade triggered by solar radiation intercepted by plant canopies, which provides energy for the photosynthesis process. The latter gives rise to a potential production of glucose that is gradually curtailed according to various kinds of losses (translocation from photosynthetic to storage organs, maintenance and production respiration, temperature and water limitations, etc.) up to reaching a final production. The selected approach is widely adopted by multi-crop production models [42,43].

More in detail, the first modelling step is the estimate of the daily global solar radiation Gsr by

$$\mathrm{Gsr} = \mathrm{Csr} \cdot \mathrm{Sf} \quad [\mathrm{MJ\ \ m-2\ \ d-1}], \tag{1}$$

where Csr is the clear sky radiation that is the maximum radiation with clear sky conditions for a given latitude and day of the year (doy). Csr and other model outputs are originally carried out for the 15th day of each month and monthly values are simply carried out multiplying them for the days of the month (dom).

Photosynthetic output for a given Gsr and CO_2 level is produced with the Totass model [44], which implements the Goudriaan and van Laar Gaussian integration method used to integrate instantaneous assimilation rates over the canopy and over the day [45]. This subroutine calculates daily total gross assimilation (Gass) by performing a Gaussian integration over time. At three different times of the day, radiation is computed and used to determine assimilation where integration takes then place.

The potential net assimilation Pna of crops is obtained by:

$$\mathrm{Pna} = \mathrm{Gass} \cdot (1 - \mathrm{Mres}) \quad [\mathrm{g\ \ m-2}], \tag{2}$$

where the multiplier coefficient Mres, which ranks in the 0–1 range, describes the losses related to respiration and translocation of photosynthetic products from the green organs towards the storage ones and is simulated by means of the following empirical equation:

$$\mathrm{Mres} = 0.0003 \cdot {T_{\mathrm{m}}}^2 + 0.0062 \cdot T_{\mathrm{m}} + 0.1027 \quad [0\text{–}1\ \text{range}]. \tag{3}$$

The temperature limitation of growth is analyzed taking into account the fact that plant growth is ruled by temperatures and that it happens in a specific range delimited by two reference temperatures, named lower cardinal LC and upper cardinal UC [1]. In this range it is possible to recognize an optimal sub-range (delimited by lower optimal LO and upper optimal UO) where growth happens without thermal limitation. In the light of this, the plant response to a given temperature T_{d} is modelled with the parameter TL, linearly growing from 0 to 1 between LC and LO, equal to 1 between LO and UO and linearly decreasing from 1 to 0 between UO and UC. This temperature limitation model is applied to hourly data produced with the de Wit model [46] applied to T_{x} and T_{m} and the monthly limitation $\mathrm{TL_m}$ is obtained as arithmetic mean of the 24 hourly values.

The lower cardinal is also used to calculate monthly thermal resources expressed as growing degree days [47]:

$$\mathrm{Gdd_m} = \mathrm{dom} \cdot (T_{\mathrm{m}} - \mathrm{LC}) \quad [^{\circ}\mathrm{C}], \tag{4}$$

where a value of 0 is imposed to $\mathrm{Gdd_m} < 0$. Growing degree days cumulated from the sowing date (gddcum) are used both to detect the date of harvest that is carried out when cumulated gddcum overcome the prescribed threshold (gddcum_harvest —see table 1) and to detect the leaf area index (LAI) in the following way:

$$\mathrm{LAI} = \mathrm{gddcum}/200 \quad [^{\circ}\mathrm{C}]. \tag{5}$$

Water limitation factor $\mathrm{WL_{fr}}$ has been estimated for a soil layer explored by roots with the following hydrologic parameters: water content of 250 mm at field capacity (fc) and 100 mm at permanent wilting point (wp), which means

Table 1. Parameterizations of production model for WMRS.

	Wheat	**Maize**	Rice	Sybean
Kc_ini	0.4	0.2	0.2	0.27
Cmin	5	8	13	10
COPTinf	17	25	28	23
COPTsup	25	32	31	35
Cmax	32	34	38	36
Gddcum_harvest	1700	1500	1300	1200
Maximum rate of leaf photosynthesis[(a)]	40	40	30	40
HI	0.5	0.5	0.5	0.5
Beginning of cropping cycle for boreal hemisphere (month)	October	March	March	March
End of cropping cycle for boreal hemisphere (month)	July	November	November	November
Beginning of cropping cycle for austral hemisphere (month)	April	September	September	September
End of cropping cycle for austral hemisphere (month)	January	May	May	May

[(a)] Plmx [45].

a maximum water reservoir of 150 mm refillable by precipitation or irrigation. The following continuity equation (mass conservation for water) was applied to this reservoir:

$$\mathrm{WC_{m+1}} = \mathrm{WC_m} + P_\mathrm{m} - \mathrm{ET_0} \cdot \mathrm{k_c} - \mathrm{inf} \quad [\mathrm{mm}], \tag{6}$$

where WC is the soil water content respectively at month m and m − 1, $\mathrm{ET_0}$ is the reference crop evapotranspiration calculated with the Hargreaves and Samani method [41], the infiltration inf expresses the loss of water that exceeds the capacity of the reservoir and the crop coefficient $\mathrm{k_c}$, used to obtain the crop maximum evapotranspiration ($\mathrm{ET_m}$) from $\mathrm{ET_0}$, is expressed as

$$\mathrm{kc} = \mathrm{kc\_ini} + \mathrm{LAI}/5.5, \tag{7}$$

where kc_ini is the initial crop coefficient adopted at sowing.

Once the soil water content WC at a given time is obtained, $\mathrm{WL_{fr}}$ is obtained by means of the following algorithm:

$$\mathrm{WL_{fr}} = (\mathrm{WC\text{-}wp})/(\mathrm{wccr\text{-}wp}), \tag{8}$$

where wccr (threshold of sensitivity to water deficit) is obtained as

$$\mathrm{wccr} = \mathrm{wp} + (1 - \mathrm{dp}) \cdot (\mathrm{fc\text{-}wp}), \tag{9}$$

where the soil water depletion factor dp describes how easy it is to extract water from the soil as a function of $\mathrm{ET_0}$ (in its turn function of the atmospheric demand of water) and is expressed as

$$\mathrm{dp} = \mathrm{ts}/(\mathrm{ts} + \mathrm{ET_0}), \tag{10}$$

where the value 9.0 has been assigned to the characteristic potential transpiration rate ts [47].

The partial effect of irrigation on maize, rice and soybean is simulated imposing the rule that $\mathrm{WL_{fr}}$ for these crops cannot be lower than 0.50, while this rule is not adopted for wheat that is generally a rain fed crop.

Therefore, the final monthly production is given by

$$\mathrm{DMI_{fin}} = \mathrm{PNA} \cdot \mathrm{TL_m} \cdot \mathrm{WF_{fr}} \cdot \mathrm{HI} \cdot \mathrm{MI} \cdot \mathrm{dom} \quad [\mathrm{t\,ha^{-1}\,m^{-1}}], \tag{11}$$

where HI is the harvest index adopted to convert total crop dry weight into useful product weight and the management intensity factor MI [16] is related to technology (genetics and management of biotic and abiotic stresses) and will be described in the paragraph devoted to calibration. Table 1 summarizes the values of the model parameters adopted for WMRS crops.

Table 2. Basic scenarios adopted for this work. Temperatures and atmospheric CO_2.

	Scenarios				
	Glacial	Pre-industrial	Today	Future_1	Future_2
Monthly and yearly temperatures - difference from today values (°C)	−6	−1	0	+2	+4
CO_2 (ppmv)	180	280	400	560	800

Table 3. Percentage distribution of WMRS crops (Cd%) for the three selected climatic belts.

Climate	Yearly mean temperature	Wheat	Maize	Rice	Soybean
Tropical	$> 20\,^{\circ}$C	0	40	50	10
Warm temperate	> 8 and $\leq 20\,^{\circ}$C	20	40	25	15
Cold temperate	≥ 4 and $\leq 8\,^{\circ}$C	100	0	0	0

2.3 Parameterizations for the five reference scenarios

The thermal and CO_2 scenarios adopted for WMRS crops are reported in table 2. The run of the production model is founded on the working hypotheses that only yearly crops (winter wheat, maize, rice and soybean) are adopted while intermediate crops [48] are avoided.

A realistic distribution of the four selected crops on the world agricultural areas is difficult to obtain because it is affected by a strong inter-yearly variability as a function of many factors, like prices, machinery, irrigation water availability, climate and soil characteristics and farmers habits and skills. More in detail, many cropping systems [48] that involve a large number of crops are adopted in different agricultural areas. In the light of the above-mentioned situation, the five basic scenarios were produced on the basis of the agro-ecological rules of crop distribution shown in table 3.

Wheat is the only crop among WMRS that is suitable for cold temperate climates while in many cases it is unsuitable for tropical areas due to its peculiar physiology (it is a long day crop and many varieties need vernalization). Furthermore maize, rice and soybean are unsuitable for cold temperate climates.

The water limitation parameter WLfr for wheat can range from 0 to 1 while only the range 0.5–1 is allowed for maize, soybean and rice, in order to take into account the coexistence of rainfed and irrigated crops.

The area of each model cell occupied by each crop is given by

$$\mathrm{Acrop} = \mathrm{cell\_area} \cdot \mathrm{Ar\%} \cdot \mathrm{Cd\%} \cdot \mathrm{WMRS\%} \quad [\mathrm{ha}], \tag{12}$$

where Ar% is the percentage of each cell occupied by arable crops from EarthSat database[1], % WMRS is the percentage of WMRS on total crop area (45.7% for 2013) and Cd% is the crop distribution reported in table 3.

The five above-described basic scenarios were used to generate some derived scenarios, respectively, characterized by the absence of water limitation and agricultural land expansion towards North in the North Hemisphere. The scenarios without water limitation were obtained adopting the rule $\mathrm{WL_{fr}} = 1$ for WMRS crops while agricultural land expansion towards North was obtained only for future_1 and future_2 scenarios, assuming a standard value (15% for future_1 and 25% for future_2) for cells located at latitudes above 55 °N and altitudes below 500 m asl, where agricultural land is, respectively, less than 15% and 25% of the total cell area.

2.4 Model calibration, verification and sensitivity analysis

The model was parameterized with data coming from van Keulen and Wolf [49], University of Illinois [48] or from author's experience and reported in table 1. Once it was parameterized, the model was tuned with reference to current technological conditions by means of the MI factor,

$$\mathrm{MI} = 1 - (\mathrm{V_{sim}} - \mathrm{V_{mea}})/\mathrm{V_{mea}} \quad [\mathrm{ha}], \tag{13}$$

where $\mathrm{V_{sim}}$ are values simulated before tuning and $\mathrm{V_{mea}}$ are global productions for 2013 [27].

Model verification was carried out with reference to some States of the USA for which long time series of crop yield (from 1895 for maize, wheat and rice, from 1924 for soybean) are available in the USDA datasets[2], while the

[1] `http://www.earthstat.org/data-download/`.

[2] `https://quickstats.nass.usda.gov`.

Table 4. Time series and other details of verification.

Crop	State	Producton time series	NOAA NCDC time series	Detrending period	Linear trend equation	HI
Wheat	Kansas	1895-2016	Statewide	1956-2016	$y = 0.0138x + 1.528$ (R^2 0.3282)	0.65
Maize	Iowa	1895-2016	Statewide	1937-2016	$y = 0.0297x + 0.738$ (R^2 0.9222)	0.50
Rice	Louisiana	1895-2017	South-Central	1946-2016	$y = 0.0558x + 1.746$ (R^2 0.944)	0.25
Soybean	Iowa	1924-2016	Statewide	1924-2016	$y = 0.1072x + 2.2254$ (R^2 0.892)	0.25

time series (values for the whole state or for quadrants of it) of the weather variables that drive the model (monthly mean temperature and precipitation) are available in the NOAA-Ncdc datasets[3]. More specifically, the model was verified with corn and soybean data from Iowa, one of the States of the Corn Belt, where these crops are most widely present and the flatness of the territory enhances the representativeness of statewide weather data. With reference to rice, the State of Louisiana, the third main producer in the USA, was preferred to the first two (Arkansas and California), because the technological trend of measured yield can be easily interpolated by a linear equation and the representativeness of the weather time series available for the South-Central part of the State is enhanced by the flatness of the land. Kansas was adopted for wheat because it is the second main producer in the USA and the representativeness of weather data is enhanced by the relative homogeneity of its Eastern part.

The choice to work with data of whole states or relevant parts of them gives errors, due to the space and time variability of crop production and weather driving variables but, at the same time, it gives an analysis that is representative of the spatial scale selected for this work.

Measured yield data need to be pre-processed before the comparison with simulated ones, because their time variability is mainly the result of the superimposition of tree distinct phenomena:

- the technology trend started, in the USA, between the 30 s and the 40 s of the 20th century [50] and is caused by improvement in genetics and cropping techniques, like tillage methods, fertilizing, pest an diseases management and harvesting;
- the weather effect that gives origin to a typical inter-annual variability;
- the CO_2 trend, due to the growing fertilizing effect of carbon dioxide.

On the other hand, simulated yields are only affected by the CO_2 trend and the weather effect, whereby they must be compared with measured yields detrended from the technology trend. The latter was estimated by linear interpolation (table 4) applied to time series preliminarily detrended from CO_2 effect on yield estimated by means of the following logarithmic equation [44]:

$$Ax = 1 + B * \ln(Cx/C0), \tag{14}$$

where Ax is the rate of increase of crop yield for the year x with reference to the base year 0, while C0 and Cx are the CO_2 atmospheric level (ppmv) for the same years and the B parameter, defined by Penning de Vries *et al.* [44], is 0.8 for the C3 plants (wheat, soybean and rice) and 0.4 for the C4 species (maize).

All the gathered datasets were adopted for comparisons with the only exception of the 1993 yield of maize, omitted because it was negative after the technology detrending.

Verification results were evaluated by means of the Pearson correlation coefficient and the two mean absolute error (MAE) and mean bias error (MBE) indices, which are used to describe the differences between simulated and observed/detrended yields. MAE measures the total spread while MBE (average differences were positive and negative differences summed together potentially to cancel) measures the skewness of simulated yields toward either overpredictions or under-predictions (see table 5).

The sensitivity analysis is useful to evaluate the domain of applicability of the model and it was carried out on the model detrended for technology and executed with water limitation on the whole Iowa time series of meteorological data (1895–2016). More specifically, the sensitivity to temperature was evaluated by adding a constant additive term to real values, which allows us to evaluate how the model behaves under extreme thermal conditions.

From the verification and the sensitivity analysis of the model we can deduce that the model, though operating with a monthly time step and with a low number of parameters, is able to capture in a sufficiently accurate way the variability induced by CO_2 and temperature and, therefore, it is useful to meet with the objective of this work.

[3] `http://www.ncdc.noaa.gov/cag/time-series/us`.

Table 5. Mean absolute error MAE, mean bias error MBE and Pearson correlation coefficient r between simulated and observed/detrended yield.

Crop	Simulated average (t/ha)	Measured average (t/ha)	MAE (t/ha)	MBE (t/ha)	Pearson correlation coefficient r	Pearson coefficient of determination r2
Wheat	1.33	1.37	0.4417	−0.0455	0.38974[(a)]	0.15190
Maize	2.63	2.67	0.5652	−0.0198	0.60741[(a)]	0.30561
Rice	2.37	2.31	0.4522	0.06750	0.56453[(a)]	0.31870
Soybean	0.93	0.94	0.1725	−0.0099	0.46934[(a)]	0.22296

[(a)] Confidence level above 99%.

Table 6. Calibration coefficient c_coeff for the four selected crops obtained in function of present measured Vmea and simulated Msim global productions of WMRS crops (million t).

Crop	V_{mea}	V_{sim}	c_coeff
Wheat	724.3	1011.0	0.60
Maize	1008.1	1374.4	0.64
Rice	732.1	1006.5	0.63
Soybean	291.3	378.0	0.70

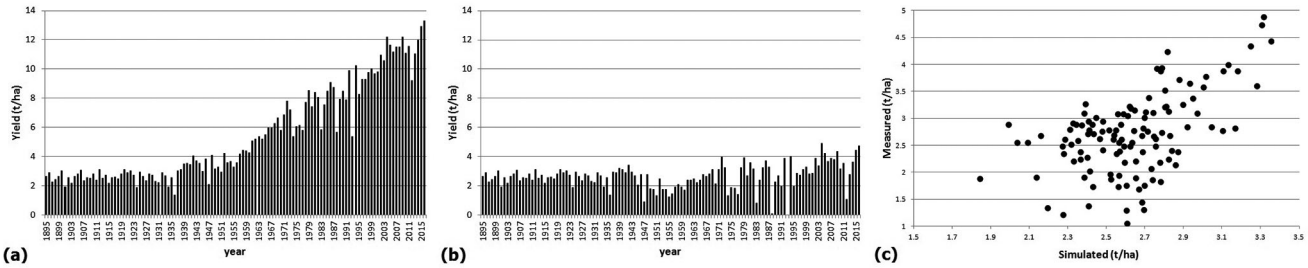

Fig. 1. The original time series 1985–2016 of maize yield in Iowa is represented in (a). Please note the strong technology trend. In (b) is represented the technology-detrended-measured time series used for correlation analysis with simulated values. Finally the scatterplot of simulated *vs.* technology-detrended-measured values is shown in (c) where only CO_2 trend and weather induced variability are evident.

3 Results

3.1 Model calibration, verification and sensitivity analysis

The values of the coefficient c_coeff that express the weight of limitations not simulated by the model (nutrient limitations and effects of biotic and abiotic stresses) are reported in table 6. Let us note that the values are in agreement with the most recent estimates of crop losses by pests, weeds and pathogens on wheat and maize, respectively, equal to 34.0% and 38.3% for the 1988–1990 and 28.2% and 31.2% for the 2001–2003 periods [51].

In order to adapt the model to USA cropping conditions before the beginning of the technology trend, the c_coeff assigned to WMRS was, respectively, 0.17, 0.30, 0.32 and 0.12 in order to express the effect of the archaic technologies adopted before the beginning of the Green Revolution.

The main phases of the work conducted for maize are reported in fig. 1 while the same phases for wheat, rice and soybean are represented in figs. S2, S3 and S4. The good agreement between observed and simulated values is testified by the highly significant Pearson r, low MAE and very low MBE.

Verification activity shows that the model adopted explains 15% (wheat), 31% (maize), 32% (rice) and 22% (soybean) of the total yield variability. These data are in agreement with the results of:

– Ray *et al.* [52], who, working on WMRS data for the period 1979–2008 and 13500 political units, showed that climate variations explain about a third of the global yield variability.
– Muller *et al.* [53], who, comparing the results of 14 global gridded simulation models for the reference period 1982–2006 with FAO data, obtained r2 coefficients between 0.14 and 0.45 for wheat (for the 10 models achieving

Table 7. Output of the 5 standard scenarios —basic run (million t).

	Scenarios				
	Glacial	Pre-industrial	Today	Future_1	Future_2
Wheat	363	558	573	408	336
Maize	339	666	928	1266	1457
Rice	262	468	558	657	727
Soybean	169	226	275	351	378
total	1133	1918	2333	2682	2897
% on today scenario	49	82	100	115	124

a highly significant correlation on a total of 14); between 0.18 and 0.79 for maize (for the 13 models achieving a highly significant correlation on a total of 14); between 0.17 and 0.41 for soybean (for the 7 models achieving a highly significant correlation on a total of 13); between 0.34 and 0.47 for rice (for the only 2 models that achieved a highly significant correlation on a total of 11).

Results of the sensitivity analysis for temperatures are summarized in fig. S5, which shows average yields and average $+/-1$ standard deviation for WMRS crops during the 1895–2016 period. These data were obtained working on 20 synthetic temperature time series produced adding a set of unitary values in the range between -10 and $+10$ to the Iowa time series. The sensitivity analysis highlights that average yields show a maximum at temperatures between -2 and $-3\,^{\circ}$C compared to today, for corn, between -2 and $+1\,^{\circ}$C for rice, between -3 and -4 for wheat and between -3 and -2 for soybean. The likely cause of this phenomenon is that the model sets the harvest date when the thermal threshold defined in table 3 is exceeded. As a result, the duration of the cycle is prolonged with lower temperatures and this enables a longer period of accumulation of dry matter into the kernels. Far from being an artifact of the model it is a real phenomenon as shown for example by soft wheat that in England (yearly TD at sea level of about $10\,^{\circ}$C) can exceed 10 t/ha while, in Italy (yearly TD of 13–18 °C), the maximum production is about 8 t/ha.

Results of the sensitivity analysis for precipitation are summarized in fig. S6, which shows average yields and average $+/-1$ standard deviation for WMRS crops during the 1895–2016 period. These data were obtained working on 13 synthetic time series of precipitation generated multiplying the Iowa time series for a coefficient between 0.3 and 1.5 with step 0.1. In this case crop production of WCRS shows a gradual increase with the growth of rainfall from 30% to 150% of the real values.

3.2 Scenarios

Results of the model run for the five base scenarios are listed in table 7. These data show that the return to a glacial period would reduce by 51% the global productivity for thermal (low temperatures) and nutritional (low levels of CO_2) reasons. The crop most affected by yield drop is maize (from 928 to 239 billion of t; −63%) while the less affected is wheat (from 573 to 363 billion of t; −37%). Similarly, the return to pre-industrial conditions would reduce global production of WMRS by 18% from today's values.

Furthermore future base scenarios would lead to an increase in WMRS yields of 15% from today for future_1 and 24% for future_2.

More specifically, for scenarios future_1 and future_2, wheat production decreases, respectively, to 71% and 59% of the present values while the more thermophilic summer crops increase their production (respectively, +36 and +57% for maize, +18 and +30% for rice and +28 and +37% for soybean).

The latitudinal distribution of crop production with base scenarios (fig. 3(a)) shows the determinant contribution of mid-latitudes of the North Hemisphere to global food production that is further emphasized by the increase of CO_2 and temperatures. Simulations with expansion of crops towards North (table 8) show that, for scenarios future_1 and future_2, the latitudinal contribution is significant until 74 °N overcoming the polar circle while for today conditions a significant production is obtained only until 63 °N (a little below the polar circle). The North expansion, for scenarios future_1 and future_2, for wheat and maize is also highlighted by maps in figs. 2(a), (b).

Vice versa, the glacial scenario shows a relevant latitudinal contraction of crops in the North hemisphere where production is significant only until 52 °N, a latitude that is reached thanks to the mitigating effect of oceans that, for example, allowed the presence of the early *Homo sapiens sapiens* (Cro-Magnon man) in France during the Wurm glaciation [54].

Figure 3(a), (b), (c) highlights that the austral hemisphere shows a low sensitivity to the change of scenarios. On the other hand, if this hemisphere shows a low sensitivity to global temperature variations due to the strong oceanic influence its contribution to global production of WMRS is secondary due to the low presence of lands.

Table 8. Output of the 5 standard scenarios —run with agricultural land expansion towards North (million tons).

	Scenarios				
	Glacial	Pre-industrial	Today	Future_1	Future_2
Wheat	363	558	573	489.4	460
Maize	339	666	928	1268	1547
Rice	262	468	558	657.4	746
Soybean	169	226	275	352.2	404
total	1133	1918	2333	2767	3157
% on today scenario	49	82	100	119	135

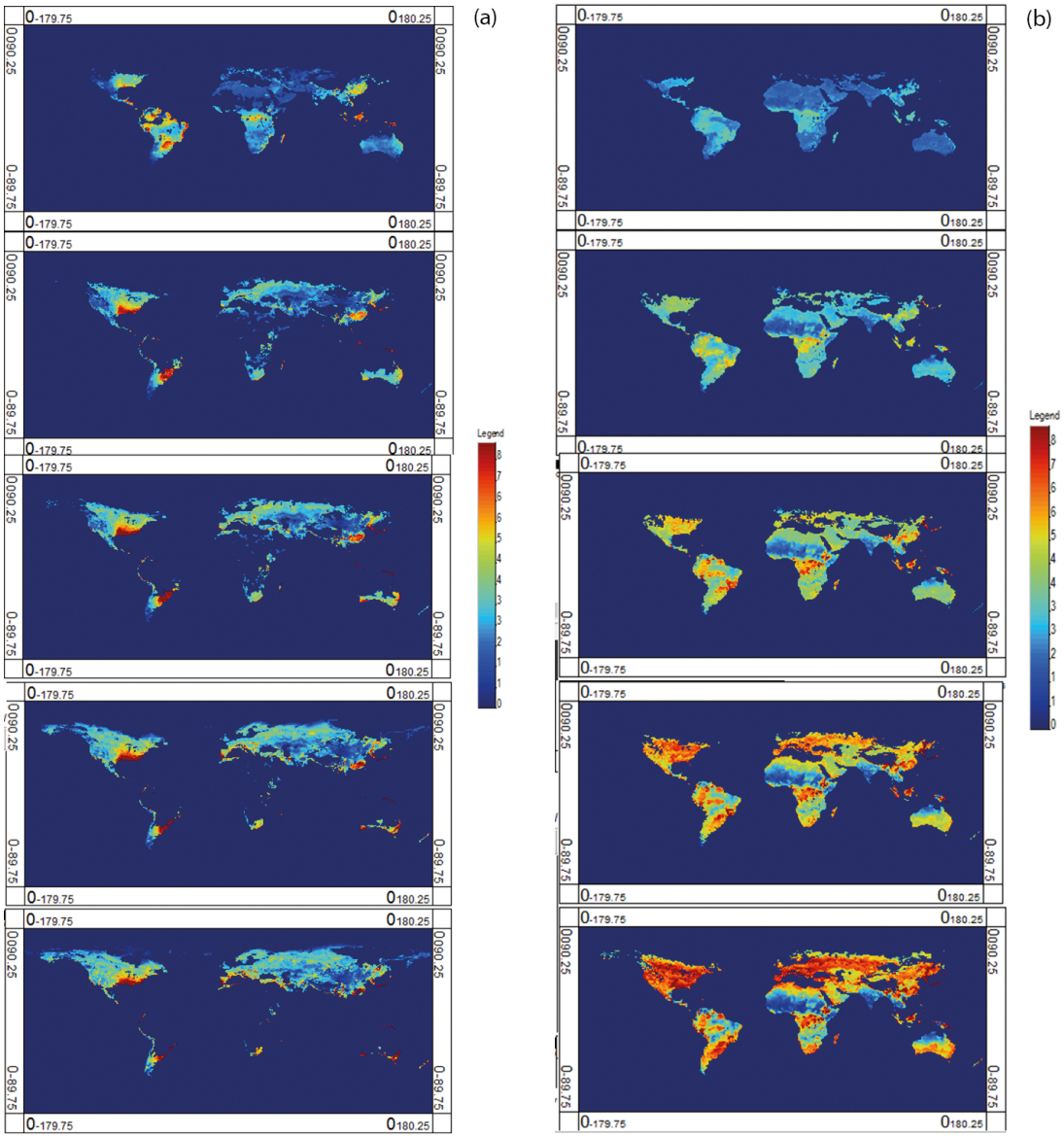

Fig. 2. World maps of wheat (a) and maize (b) production for the five scenarios listed from above to below in the sequence glacial, pre-industrial, current, future_1, future_2.

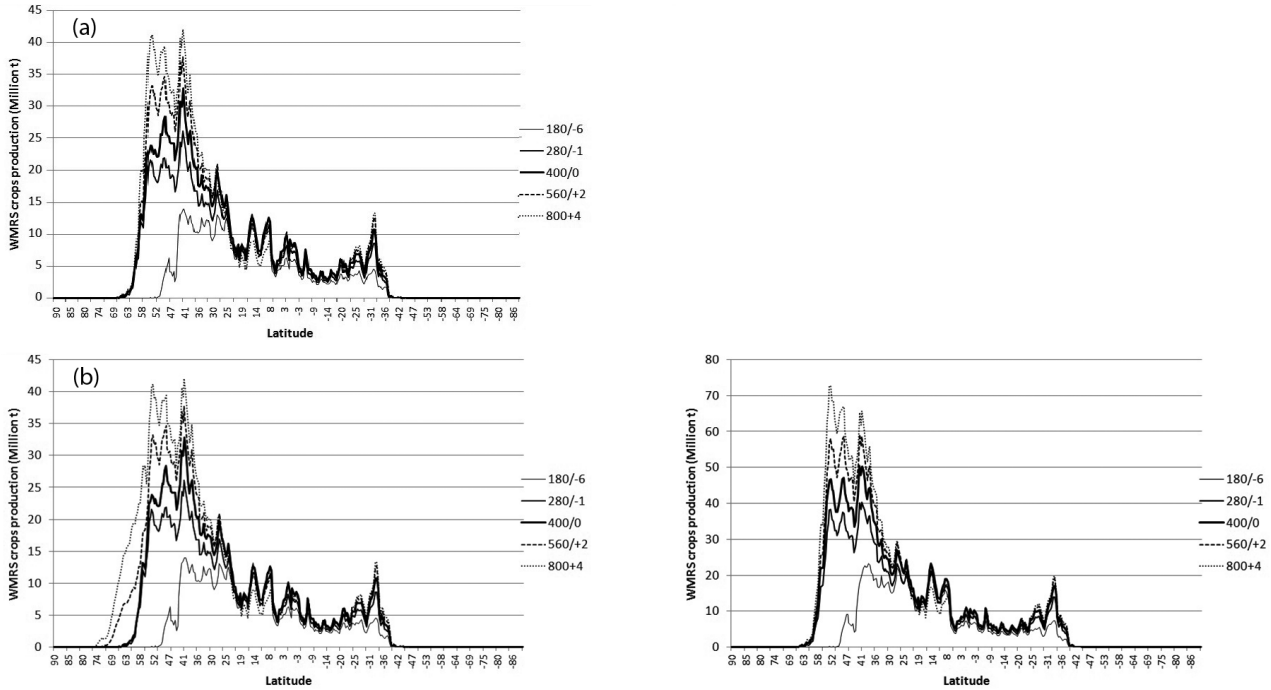

Fig. 3. Latitudinal distribution of crop production for the five scenarios. Values are total productions of each belt of 0.5° lat: (a) Base scenarios; (b) scenarios with latitudinal expansion toward North; (c) scenarios without water limitation.

Table 9. Output of the 5 standard scenarios —run without water limitation (million tons).

	Scenarios				
	Glacial	Pre-industrial	Today	Future_1	Future_2
Wheat	689.8	1122.2	1154.4	801.6	675.5
Maize	454.3	938.6	1324.5	1847.2	2167.2
Rice	345.5	633.9	758.8	901.1	1020.2
Soybean	223.5	320.6	393.7	513.3	563.5
total	1713	3015	3631	4063	4426
% on today scenario	47	83	100	112	122
% on basic scenario (with water limitation)	151	157	156	151	153

Finally the simulations carried out without water limitation (table 9) give a systematic increase in production of WMRS crops (more than 50% for all scenarios). This highlights the central role of water limitation in crop production and the importance of irrigation in order to ensure global food security. In fact, irrigated agriculture represents 20 percent of the total cultivated land, but contributes 40 percent of the total food produced worldwide [27]. The global results obtained with the 5 scenarios and the 3 super-scenarios are presented in fig. 4.

4 Discussion

The five selected scenarios show that the return of temperature and CO_2 to glacial or pre-industrial values would give rise to serious disadvantages for food security and should be as far as possible avoided, as also highlighted by the results of Sage and Coleman [28] and Araus [29].

Furthermore the future scenarios future_1 and future_2 should be evaluated with reference to the general objective of increase of 50–70% in the global food production stated by FAO in order to feed the 9.7 billion of people foreseen for 2050 [55,56]. From this point of view, it can be considered that the increase of temperature and CO_2 (future_1 and future_2 base scenarios) in a *ceteris paribus* perspective (steady state of cultivated surfaces, genetics and technologies) is clearly insufficient to meet the rise of the global population. On the other hand, if the basic scenarios are enriched with the expansion of irrigation and the northward shift of WMRS crops, this objective could become reachable also in the absence of other forms of innovation.

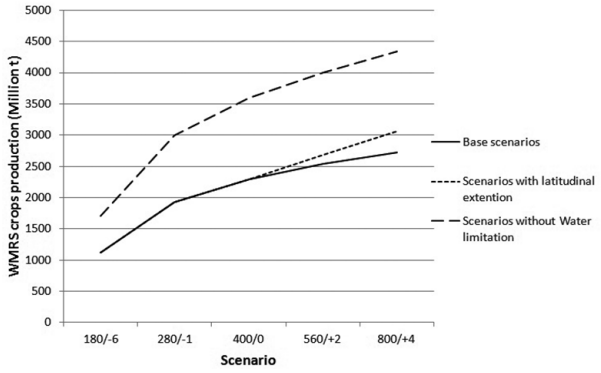

Fig. 4. Match among the 3 super-scenarios (base, with latitudinal expansion and without water limitation).

However it must be said that our future scenarios have not considered:

- The negative effect on crops of extreme events like droughts, rainfall excess, frost and heat waves, which are beyond the scope of a model that operates on thirty-year average data.
- The future perspective of the strongly positive technological trend that during the 20th century produced an increase of yields of WMRS crops of 400–600% [24], outclassing other causal effects. It is quite difficult to state if and to what extent this trend will prosecute because it depends on a series of social, economic and cultural factors whose evaluation is prohibitive in the light of the extreme variety that characterizes the 590 million farms of the world. In any case a crucial role will be played by the activities of research and technology transfer.
- The implementation of strategies of adaptation based on i) changes in crops (*e.g.*, from maize to sorghum, another C4 crop that is more tolerant to drought); ii) changes in varieties (*e.g.*, the maize hybrids are classified in FAO classes from 100 to 800 and more on the base of their earliness; therefore, a late hybrid like a class 700 in comparison with an earlier one like a class 400 needs a longer growth period but at the same time is much more productive); iii) changes in cropping techniques (*e.g.*, fertilization, crop protection) [37].
- The improved resistance to drought of crops grown with higher CO_2 levels [4].
- The enhanced availability of iron in calcareous soils for all the non graminaceous monocots and dicots under elevated CO_2 [57] with reduction of the Iron Deficiency Chlorosis disease that affect sensitive crops on the 30% of the Earth surface [58].
- The adaptation potential existing in the improvement in genetics (new varieties and species able to adapt to new climates and higher CO_2 levels) [37].
- The intrinsic incertitude of the thermal scenarios future_1 and future_2 adopted in this work. This is because over the last two decades the observed rate of increase in global-mean surface temperature has been at the lower end of rates simulated by CMIP5 GCM models, with a hiatus that IPCC AR4 in chapter 9 and 11 [4] attributes to a decline in the rate of increase in aerosol effective radiative forcing (ERF) and a cooling contribution from internal variability.

Another important question is given by the effect of CO_2 growth on crop quality. For instance Myers *et al.* [59] claimed that wheat roots under elevated CO_2 absorb a lower quantity of $NO3^-$ and by consequence production is higher but protein content of grain is lower. So they deduced that increasing CO_2 threatens human nutrition. In my opinion the relevance of this problem was probably exaggerated because nitrogen nutrition of wheat can be guaranteed directly through the leaves (foliar fertilization) with the great advantage of avoiding the energy loss due to the transformation of NO_3 in NH_4 by means of the nitrate reductase [60]. Moreover the problem of proteins availability for human diets could be easily overcome reducing wheat production and increasing surfaces at soybean and other leguminous crops which unlike non-leguminous C3 plants have the potential to maximize the benefit of elevated CO_2 by matching stimulated photosynthesis with increased N_2 fixation by symbiotic bacteria leaving in their root nodules [61].

The adaptation derived from irrigation expansion was highlighted showing that irrigation is a powerful tool in order to increase crop production in quantity an quality and could be particularly effective if carried out with irrigation systems with high water use efficiency (drip and microjet irrigation, subirrigation, center pivots, raingers and so on) which can be used also for foliar fertilization, pesticides distribution and mitigation of high and low temperatures.

The adaptation potential derived from the cropland expansion towards Boreal territories of America and Eurasia should be enhanced by means of land reclamation activities [49] compatible with needs of protection of natural ecosystems.

By a general point of view the proposed scenarios are an exercise useful to evaluate the effects of different limitations on crop growth and to give to the reader a perspective useful for planning the future development of the agricultural sector on a global scale. By the way the proposed approach overcomes the limitation of the results presented in

chapter 7 of the IPCC AR5 report [4] which review of the past and foreseen effects of climate change on agriculture (see figs. 7.2 and 7.5) was carried out by combining the results of models that only in some cases evaluate the fertilizing effect of CO_2 and moreover operate with different technologies (physiological process-based and statistical models), for different emission scenarios and at different time and space scales.

5 Conclusions and future developments

The simulated scenarios show that the agricultural sector is able to successfully meet the challenge of global change and guarantee food security to levels higher than the current ones for a world population that in 2050 will exceed 9 billion people. Such a perspective will be realized, however, only if a lot of strategic decisions in the fields of genetics, reclamation of lands in northern latitudes, expansion and efficiency improvement of irrigation and reduction of losses due to biotic and abiotic stresses will be adopted.

In this context the proposed modelling approach could be interesting in order to evaluate the mitigation potential existing in a better exploitation of agriculture as carbon cycle regulator. This should be pursued considering agriculture not only as a tool for storing carbon into the soil (whith a quite positive effect on fertility) but also as a producer of biological polymers for industrial chains (energy, plastics, drugs and so on) that at present are fed by fossil fuels. About this latter statement we should consider that during years of overproduction at global scale the systematic use of agricultural products for extra-agricultural purposes is an interesting perspective, of course if it does not interfere with food security. The same thing is true for agricultural byproducts that should be used for extra-agricultural purposes if they do not reduce soil organic matter. These strategies are particularly interesting because they can be implemented very quickly in agriculture in the light of the high flexibility and rapidity of response of farms.

References

1. W. Larcher, *Physiological Plant Ecology*, 3rd edition (Springer, Berlin, 1995) p. 506.
2. N.T. De Saussure, *Recherches Chimiques sur la Végétation* (Chez la Veuve Nyon, Librairie, 1804) p. 327.
3. A.V. Barker, D.J. Pilbeam (Editors), *Handbook of Plant Nutrition* (CRC press, Taylor and Francis Group, 2015) p. 747.
4. T.F. Stocker, D. Qin, G.K. Plattner, M. Tignor, S.K. Allen, J. Boschung, A. Nauels, Y. Xia, V. Bex, P.M. Midgley (Editors), *IPCC, Climate Change 2013: The Physical Science Basis*, contribution of Working Group I to the *Fifth Assessment Report of the Intergovernmental Panel on Climate Change* (Cambridge University Press, Cambridge, UK and New York, NY, USA, 2013) p. 1535.
5. S. Arrhenius, *Worlds in the Making: The Evolution of the Universe* (Harper, 1908) p. 258.
6. A. Menozzi, U. Pratologo, *Manuale di Chimica Vegetale e Agraria*, Vol. **I**, *Chimica vegetale* (Hoepli, Milano, 1945) (in Italian).
7. H.T. Brown, F. Escombe, Philos. Trans. R. Soc. London, Ser. B **193**, 223 (1900).
8. E. Demoussy, C. R. Acad. Sci. Paris **883** (1904) (in French).
9. H. Fischer, *Pflanzenernährung mittels Kohlensäure, Gartenflora*, Heft **14** (1912) (in German).
10. E. Reinau, *Praktischen Kohlensäuredüngung in Gärtnerei und Landwirtschaft* (Springer, Berlin, 1927) (in German).
11. S. Tonzig, E. Marré, *Elementi di botanica*, Vol. primo, parte seconda (1968) p. 1581 (in Italian).
12. C. Stanghellini, F.L.K. Kempkes, L. Incrocci, Acta Hortic. **807**, 135 (2009).
13. U. Helldén, C. Tottrup, Glob. Planet. Change **64**, 169 (2008).
14. S.M. Herrmann, A. Anyambab, C.J. Tucker, Glob. Environ. Change **15**, 394 (2005).
15. S. Sitch *et al.*, Biogeosciences **12**, 653 (2015).
16. Zeng *et al.*, Nature **515**, 394 (2014).
17. R. Rafique *et al.*, Remote Sens. **8**, 177 (2016).
18. J. Wang, C. Wang, N. Chen, Z. Xiong, D. Wolfe, J. Zou, Clim. Change **130**, 529 (2015).
19. L.H. Levine, H. Kasahara, J. Kopka, A. Erban, I. Fehr, F. Kaplan, W. Zhao, R.C. Littell, C. Guy, R. Wheeler, J. Sager, A. Mills, H.G. Levine, Adv. Space Res. **42**, 1917 (2008).
20. L.H. Allen, V.G. Kakani, J.C. Vu, K.J. Boote, J. Plant. Physiol. **168**, 1909 (2011).
21. M. Wang, B. Xie, Y. Fu, C. Dong, L. Hui, L. Guanghui, H. Liu, Photosynth. Res. **126**, 351 (2015).
22. A.L. Swann, F.M. Hoffman, C.D. Koven, J.T. Randerson, Proc. Natl. Acad. Sci. U.S.A. **113**, 10019 (2016).
23. J. Diamond, *Guns, Germs and Steel. A short history of everybody for the last 13000 years* (Norton, 1997) p. 480.
24. G. Federico, *Feeding the World: An Economic History of Agriculture, 1800–2000* (Princeton and Oxford: Princeton University Press, 2005) p. 416, ISBN 069112051X.
25. J.A. Burney, S.J. Davis, D.B. Lobell, Proc. Natl. Acad. Sci. **107**, 12052 (2010).
26. A. Saltini, *Agrarian Sciences in the West*, Vol. **3**, *The course of the agrarian revolution* (Nuova terra antica, 2015) p. 409.
27. FAO, Dataset FAOSTAT3, available online at `http://faostat3.fao.org/home/E` (site visited on 12 September 2016).
28. R.F. Sage, J.R. Coleman, Trends Plant Sci. **6**, 18 (2001).
29. J.L. Araus *et al.*, J. Archaeol. Sci. **30**, 681 (2003).

30. A.A. Lacis, G.A. Schmidt, D. Rind, R.A. Ruedy, Science **330**, 356 (2010).
31. H.H. Lamb, *Climate, Present, Past and Future*, Vol. **2**, *Climatic History and the Future* (Methuen & Co Ltd., London, 1977) p. 835.
32. L. Mariani, *Applicazioni agrometeorologiche della serie storica di Mantova: possibilità e limiti*, in *Atti del convegno "Due secoli di osservazioni meteorologiche a Mantova", Ersal* (2000) pp. 191–201 (in Italian).
33. E. Le Roy Ladurie, *Histoire humaine et comparée du climat*, Vol. **I**, *Canicules et glaciers (XIIIe-XVIIIe siècles)* (Fayard, 2004).
34. C.T. de Wit, *Photosynthesis: Its Relationship to Overpopulation*, in *Harvesting the Sun*, edited by A. San Pietro, F.A. Green, T.J. Army, (Academic Press, New York, 1967) pp. 315–320.
35. J.L. Capper, R.A. Cady, D.E. Bauman, J. Anim. Sci. **87**, 2160 (2009).
36. S. Parisi, M. Bianco, L. Mariani, Ital. J. Agrometeorol. **2**, 15 (2011).
37. W. Mauser *et al.*, Nat. Commun. **6**, 8946 (2015).
38. Gray *et al.*, Nature **515**, 398 (2014).
39. M. Bernardi, Acta Tropica **79**, 21 (2001).
40. R. Leemans, W. Cramer, *The IIASA database for mean monthly values of temperature, precipitation and cloudiness on a global terrestrial grid*, Research Report RR-91-18, November 1991 (International Institute of Applied Systems Analyses, Laxenburg, 1991) p. 61.
41. R.G. Allen, L.S. Pereira, D. Raes, M. Smith, *Crop evapotranspiration—guidelines for computing crop water requirements (Irrigation and Drainage Paper 56)* (Food and Agriculture Organization of the United Nations (FAO), Rome, Italy, 1998).
42. A.K. Singh, V. Goyal, A.K. Mishra, S.S. Parihar, Curr. Sci. **104**, 1324 (2013).
43. H. Boogaard, J. Wolf, I. Supitc, S. Niemeyerd, M. van Ittersum, Field Crops Res. **143**, 130 (2013).
44. F.W.T. Penning de Vries, D.M. Jansen, H.F.M. ten Berge, A. Bakema, *Simulation of ecophysiological processes of growth in several annual crops*, in *Simulat. Monographs*, Vol. **29** (Pudoc, Wageningen, 1989).
45. J. Goudriaan, Agric. For. Meteorol. **38**, 251 (1986).
46. D.C. Reicosky, L.J. Winkelman, J.M. Baker, D.G. Baker, Agric. For. Meteorol. **46**, 193 (1989).
47. J. Doorenbos, W.O. Pruitt, *Irrigation and Drainage*, Paper No. 24. Rome (FAO, 1978).
48. University of Illinois, *Illinois Agronomy Handbook*, 23th edition (2009) available online at the following link: `http://extension.cropsciences.illinois.edu/handbook/` (site visited on 10 September 2016).
49. H. van Keulen, J. Wolf (Editors), *Modelling of Agricultural Production, Weather, Soils and Crops* (Wageningen, Pudoc, 1986) p. 479.
50. W.E. Easterling, X. Chen, C. Haysl, J.R. Brandle, H. Zhang, Clim. Res. **6**, 263 (1996).
51. E.C. Oerke, J. Agric. Sci. **144**, 31 (2006).
52. D.K. Ray, J.S. Gerber, G.K. MacDonald, P.C. West, Nat. Commun. **6**, 5989 (2015).
53. C. Müller, J. Elliott, J. Chryssanthacopoulos, A. Arneth, J. Balkovic, P. Ciais, D. Deryng, C. Folberth, M. Glotter, S. Hoek, T. Iizumi, R.C. Izaurralde, C. Jones, N. Khabarov, P. Lawrence, W. Liu, S. Olin, T.A.M. Pugh, D. Ray, A. Reddy, C. Rosenzweig, A.C. Ruane, G. Sakurai, E. Schmid, R. Skalsky, C.X. Song, X. Wang, A. de Wit, H. Yang, Geosci. Model Dev. Discuss. (2016) DOI:10.5194/gmd-2016-207.
54. B. Fagan, *Cro-Magnon: How the Ice Age Gave Birth to the First Modern Humans* (Bloomsbury Press, 2010) p. 320.
55. United Nations, *Revision of World Population Prospects*, `http://www.un.org/en/development/desa/news/population/2015-report.html` (2015) (site visited on 14 September 2016).
56. FAO, *World agriculture towards 2030/2050, The 2012 Revision*, ESA Working Paper No. 12–03, `http://www.fao.org/docrep/016/ap106e/ap106e.pdf` (2012).
57. C. Wei Jin, S. Ting Du, W. Wei Chen, G. Xin Li, Y. Song Zhang, S. Jian Zheng, Plant Physiol. **150**, 272 (2009).
58. J. Imsande, Plant Physiol. **103**, 139 (1998).
59. S.S. Myers *et al.*, Nature **510**, 139 (2014).
60. P. Khan, M.Y. Memon, M. Imtiaz, M. Aslam, Pak. J. Bot. **41**, 1197 (2009).
61. A. Rogers, E.A. Ainsworth, A.D.B. Leakey, Plant Physiol. **151**, 1009 (2009).